WARSAW UNIVERSITY OF TECHNOLOGY Index 351733
FACULTY OF CIVIL ENGINEERING
COMMITTEE FOR CIVIL AND WATER ENGINEERING
POLISH ACADEMY OF SCIENCES ISSN 1230-2945

DOI: 10.24425/ace.2023.147679

ARCHIVES OF CIVIL ENGINEERING

Vol. LXIX ISSUE 4 2023

pp. 603 –618

Research paper

Cracking risk of high-performance cement composites due to restrained autogenous shrinkage with and without soaked lightweight aggregate

Adam Zieliński[1], Anton K. Schindler[2], Maria Kaszyńska[3]

Abstract: Due to the large amount of binder and low water-cement ratio, high-performance cement composites have high compressive strength and a dense hardened cement paste microstructure. External curing is insufficient, as it cannot reach the interior parts of the structure, which allows autogenous shrinkage to occur in the inside. Lack of prevention of autogenous shrinkage and high restraint causes structural microcracks around rigid components (aggregate, rebars). Consequently, this phenomenon leads to the propagation of internal microcracks to the surface and reduced concrete durability. One way to minimize autogenous shrinkage is internal curing. The use of soaked lightweight aggregate to minimize the risk of cracking is not always sufficient. Sorption and desorption kinetics of fine and coarse fly ash aggregate were tested and evaluated. The correlation between the development of linear autogenous shrinkage and the tensile stresses in the restrained ring test is assessed in this paper. A series of linear specimens, with cross-section and length custom designed to match the geometry of the concrete ring, were tested and analyzed. Determination of the maximum tensile stresses caused by the restrained autogenous shrinkage in the restrained ring test, together with the approximation of the tensile strength development of the cement composites were used to evaluate the cracking risk development versus time. The high-performance concretes and mortars produced with mineral aggregates and lightweight aggregates soaked with water were tested. The use of soaked granulated fly ash coarse lightweight aggregate in cementitious composites minimized both the autogenous shrinkage and cracking risk.

Keywords: autogenous shrinkage of concrete, cracking risk of concrete, restrained autogenous shrinkage, early-age concrete cracking, internal curing

[1]DSc., PhD., Eng., West Pomeranian University of Technology, Faculty of Civil Engineering and Environmental, al. Piastów 50a, 70-311 Szczecin, Poland, e-mail: adam.zielinski@zut.edu.pl, ORCID: 0000-0001-7949-1831
[2]Prof., DSc., PhD., Eng., Department of Civil and Environmental Engineering, Auburn University, 237 Harbert Center, Alabama 36849, Auburn, USA, e-mail: schinak@auburn.edu, ORCID: 0000-0002-5906-2885
[3]Prof., DSc., PhD., Eng., West Pomeranian University of Technology, Faculty of Civil Engineering and Environmental, al. Piastów 50a, 70-311 Szczecin, Poland, e-mail: mkasz@zut.edu.pl, ORCID: 0000-0002-8867-6974

1. Introduction

New generation of high-performance concretes have revolutionized the concrete technology in recent years. Self-consolidating concretes replaced some ordinary concretes in prefabrication of structural elements [1] and are increasingly used in densely reinforced structures such as wall panels, columns, and beams. These concretes are characterized by higher concreting efficiency, flowability, resistance to segregation, and passing ability. The mentioned rheological properties of the mixture directly affect the durability of the element and the service life of the structure [2]. The main difference compared to ordinary concretes is the composition. More micro fillers, finer aggregate and lowering the water-cement ratio (w/c) below 0.4 require the use of efficient superplasticizers (SP) [3]. Replacing inert micro fillers with reactive mineral additives and cement allows to combine the characteristics of self-consolidating concretes with the strength and durability associated with high-performance concretes [4]. High-performance concretes with self-consolidating rheology contains high cementitious material contents and low water contents, which makes them susceptible to elevated autogenous shrinkage [5]. Restraining the free internal deformability by non-deformable components (e.g., aggregate and reinforcing bars) causes the development of micro-cracks in the material structure around rigid elements [6]. This phenomenon causes internal micro-cracks in the concrete during its maturation, that propagate to the surface which leads to reduced long-term concrete durability.

The autogenous shrinkage of cementitious composites is typically measured on linear specimens: sealed beams [7] or corrugated tubes [8]. The shrinkage strain increases as the w/c ratio decreases [9]. Although superplasticizer allow sufficient workability to be obtained in low w/c concretes, they does not directly affect the amount of autogenous shrinkage [10]. Fly ash and fillers [11] do not significantly impact autogenous shrinkage when compared to replacing cement, while blast furnace slag [12] and silica fume [9] increase the autogenous shrinkage. Holt [13] separated autogenous shrinkage from the thermal shrinkage, which is necessary at early ages when heat is liberated during the peak cement hydration period. Usage of superabsorbent polymer (SAP) [14] and shrinkage-reducing admixture (SRA) [15] up to 2% of the cement mass and usage of united expansive agent (UEA) [16] were confirmed to reduce shrinkage. The use of saturated lightweight aggregate as internal curing was effective to minimize autogenous and drying shrinkage [17]. Cracking susceptibility testing is commonly performed with the restrained ring test [18, 19], cracking-frame [20] and elliptical ring [21]. These tests assess the overall effect of restrained stress development due to both drying and autogenous shrinkage when the specimen in exposed to drying. The main parameters recorded are the steel ring strain with time and at cracking, which allows the calculation of the stress development in the concrete. A number of computer simulations of the autogenous shrinkage development and cracking time, based on probabilistic methods were carried out by others, and was proven to have reasonable accuracy [22, 23]. The restrained shrinkage ring test method (ASTM C1581) does not separately assess the free autogenous strain because only the total stress development and time to cracking is obtained from this test. Computer simulations should be validated by using material models that account for the different components that contribute to the time-depended development of

stress and strength. No studies have been found that cover how internal curing minimize the risk of cracking caused by restrained autogenous shrinkage correlated with the free autogenous shrinkage determined with specimens with matching geometries.

This paper presents results of cracking risk analyses performed for the high-performance composites using internal curing in the form of soaked lightweight aggregate–granular fly ash of various sizes. The correlation between tensile stress development results obtained from the sealed ring test specimen versus the autogenous shrinkage development in a free linear specimen is also assessed herein. In this work, sealed ring specimens were tested in accordance with ASTM C1581M-16 and free linear specimens were designed to have a cross section and length to match the geometry of the ring specimens. The development of free and restrained autogenous shrinkage as a function of time, from final setting until either cracking in the ring test specimen or up to a specimen age of 28 days, is also evaluated in this paper. The result of the analyses performed is the autogenous free shrinkage versus tensile stress correlation, assessment of the cracking risk reduction when using internal curing.

2. Experimental program

2.1. Materials and mix proportions

Various tests were performed on mortars and concretes with self-compacting rheology and with high-performance attributes. Test specimens utilized a standard portland cement (CEM I 52.5R) with a specific surface area according to Brunauer-Emmett-Teller (BET) method equal to 435 m^2/kg. Pozzolanic additives were used and included fly ash with a specific surface area of 850 m^2/kg and silica fume with a specific surface area of 19,000 m^2/kg. The effect of internal curing was assessed by using soaked lightweight aggregate made of granular fly ash in accordance with EN 13055-1. For all the concretes produced, the ratio of fine to coarse aggregate was kept at 58% by volume. The proportions of the tested cement composites (mortar and concrete) are presented in Table 1. The mass and volume ratios for individual materials are detailed in Table 2. The chemical composition of the binders used is presented in Table 3. Before testing began, the aggregate was dried at $105 \pm 2^{\circ}$C for 24 hours and next cooled for 24h. The bulk density and grain size distribution of the aggregates used are presented in Table 4.

All the aggregates used were obtained from concrete production plants. Lightweight aggregate of 4–8 mm fraction was a granulated fly ash consisting of spherical beige-brown grains with a porosity of 40 ± 3%. Samples of granulated fly ash in the coarse and fine size are shown in Fig. 1a and Fig. 1b.

Lightweight fine aggregate of 0–4 mm fraction consisted of crushed spherical aggregates. A combination of crushed aggregate particles and a high content of fine fraction provided easy access to the aggregate pores and reduced their water storing capacity. The absorption of both aggregates was tested using two methods: 1) the paper towel method, based on a test procedure from the Department of Transportation for the State of New

Table 1. Proportions of the tested mortars and concretes

Mix	Cement (kg/m^3)	Fly ash (kg/m^3)	Silica fume (kg/m^3)	Water (kg/m^3)	Internal curing water (kg/m^3)	SP (kg/m^3)	Aggregate (kg/m^3)			
							Gravel		Lightweight	
							0–2 (mm)	2–8 (mm)	0–4 (mm)	4–8 (mm)
M-0.34-NWA	725	118	59	305	–	5.5	1004	–	–	–
M-0.225-NWA	794	129	65	222	–	18	1100	–	–	–
M-0.225-LWA	794	129	65	222	54.7	18	–	–	547	–
C-0.225-NWA	462	75	38	129	–	12	642	1102	–	–
C-0.28-NWA	450	73	37	155	–	9	624	1072	–	–
C-0.28 -LWA	450	73	37	155	108	8.5	624	–	–	540

Table 2. Mass and volume ratios for individual cement composites

Symbol	Mass ratio		Volume ratio		Aggregate	
	w/c	w/b	c/a	b/a	fine	coarse
M-0.34-NWA	0.42	0.34	0.62	0.83	Gravel	–
M-0.225-NWA	0.28	0.225			Gravel	–
M-0.225-LWA					Fly ash	–
C-0.225-NWA	0.28	0.225	0.23	0.31	Gravel	Gravel
C-0.28-NWA	0.34	0.28			Gravel	Gravel
C-0.28-LWA					Gravel	Fly ash

where: w – water, c – cement, b – binder, a – aggregate.

Table 3. Chemical composition of the binders used

Binder	SiO_2	CaO	Al_2O_3	Fe_2O_3	MgO	Na_2O	SO_3	K_2O	MnO	TiO_2
CEM I 52.5R (wt.%)	20.6	65.2	4.52	2.43	1.26	0.41	3.05	–	–	–
Fly ash (wt.%)	51.0	3.60	25.8	6.02	2.62	1.17	0.38	3.12	–	–
Silica fume (wt.%)	92.8	0.29	0.48	2.20	0.21	0.34	–	0.27	0.11	0.02

York [24], and 2) pycnometry method. The first method made it possible to measure the absorption after a certain time, i.e. after 24 h. The second method allowed to determine the absorption kinetics over time. Absorption kinetics of lightweight aggregate with fractions 0–4 and 4–8 over a period of 48 hours are presented in Fig. 1c.

Table 4. Properties of the aggregate used

Parameter	Gravel fine[1] 0–2 mm	Gravel coarse[2] 2–8 mm	Crushed granular fly ash[3] 0–4 mm	Granular fly ash[4] 4–8 mm
Poured bulk density (kg/m^3)	1680 ± 40	1530 ± 30	720 ± 10	685 ± 10
Absorption capacity[5] (%)	1.2 ± 0.4	1.3 ± 0.3	9.0 ± 1.4	18.5 ± 2.1
Size (mm):	(%)	(%)	(%)	(%)
0–0.125	2.3	–	17.2	–
0.125–0.25	5.4	–	12.4	–
0.25–0.5	7.4	–	13.2	–
0.5–1	37.6	–	15.1	–
1–2	45.1	–	21.4	–
2–4	–	36.1	17.4	–
4–8	–	62.2	–	88.9

[1] oversize: > 2 mm = 2.2%,
[2] undersize: < 2 mm = 0.4%; oversize: > 8 mm = 1.3%,
[3] oversize > 4 mm = 3.3%,
[4] undersize: < 4 mm = 9.7%; oversize: > 8 mm = 1.4%,
[5] Absorption capacity after 30 minutes from pouring water on the aggregate.

The desorption test was carried out using a climatic chamber and a scale with a sensitivity of ±0.01 g. The fraction passing the 8 mm sieve and retained on a 0.25 mm sieve was tested. The desorption kinetics of lightweight aggregate 0.25–4 mm and 4–8 mm are presented in Fig. 1d. The coarse aggregate was more efficient in desorbing its moisture because in the range of 100–90% RH it desorbed 13.8% of its mass in the dry state. The lightweight fine aggregate only desorbed 11.7% of its mass in the dry state as the RH decreased from 100 to 90%. This means that the coarse aggregate will make more water available for internal curing as self-desiccation occurs due to hydration of cement. Both aggregates retained good desorption properties because a significant amount of absorbed water was released at high RH.

Additionally, the absorbability of coarse aggregate was tested three times using a water bath. The results were similar to the tests of aggregate absorption using the paper towel method and the pycnometric method. Based on these results, before making the concrete the coarse aggregate was soaked for 30 minutes and then drained for 5 minutes. According to Table 1, the extra 108 kg/m^3 of water stored in the pores of the lightweight coarse aggregate of the C-0.28-LWA concrete, constituted nearly 20% of its mass. For lightweight crushed fine aggregate soaking was achieved by adding the anticipated extra amount of water to the mixer until it obtained a constant consistency within a period of approximately 30 minutes. Finally for M-0.225-LWA, the fine lightweight aggregate was pre-soaked with 10% water

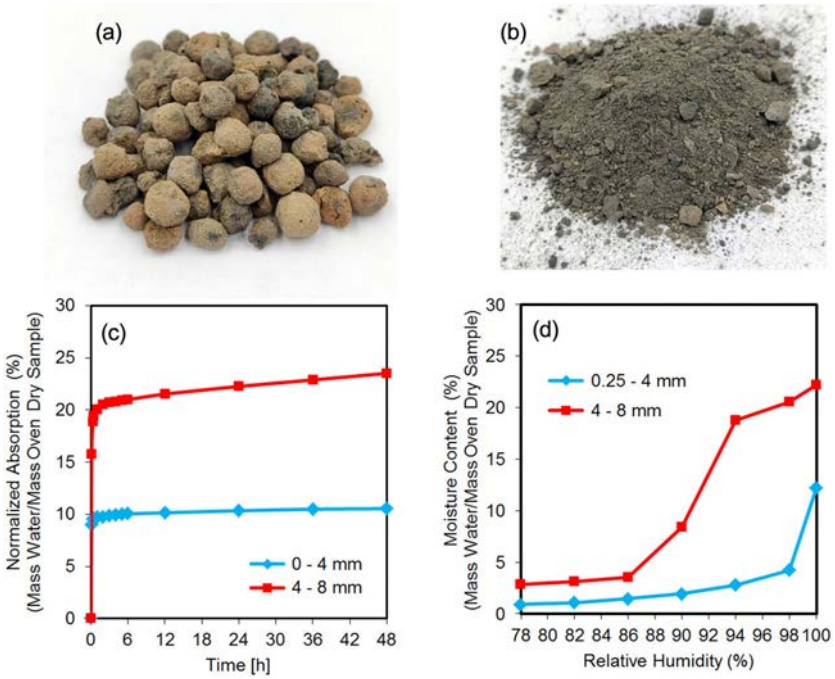

Fig. 1. Granulated fly ash: a) uncrushed coarse size 4–8 mm; b) crushed fine size 0–4 mm; c) kinetics of absorption; d) kinetic of desorption

by mass before starting with mortar preparation. The use of soaked fine and coarse fractions allowed the research team to evaluate the influence and effectiveness of granulated fly ash on internal curing and cracking susceptibility of high-performance cement composites due to restrained autogenous shrinkage.

2.2. Research methods

The rheological properties of each mixture was tested and then molded specimens. Strength test specimens after one day, were demolded and were placed in curing water at a constant temperature of 20 ± 2°C, until the day of strength testing. In the climate-control room, three ring specimens were molded to assess the or cracking susceptibility according to ASTM, and three prismatic specimens 35 × 150 × 1150 mm were made to test the free autogenous shrinkage. The length of the prismatic specimen was designed to match the circumference of the ring specimens. The concept of matching geometry in these two types of laboratory test specimens is schematically shown in Fig. 2a and Fig. 2b. In order to measure the autogenous shrinkage and its effect, the linear and ring specimens were not demolded. To eliminate friction forces, the steel rings were lubricated with oil, while the molds for the linear specimens were covered with talcum powder and the cement mixtures were molded in the foil. This way, the measurement of linear strain is equal to the

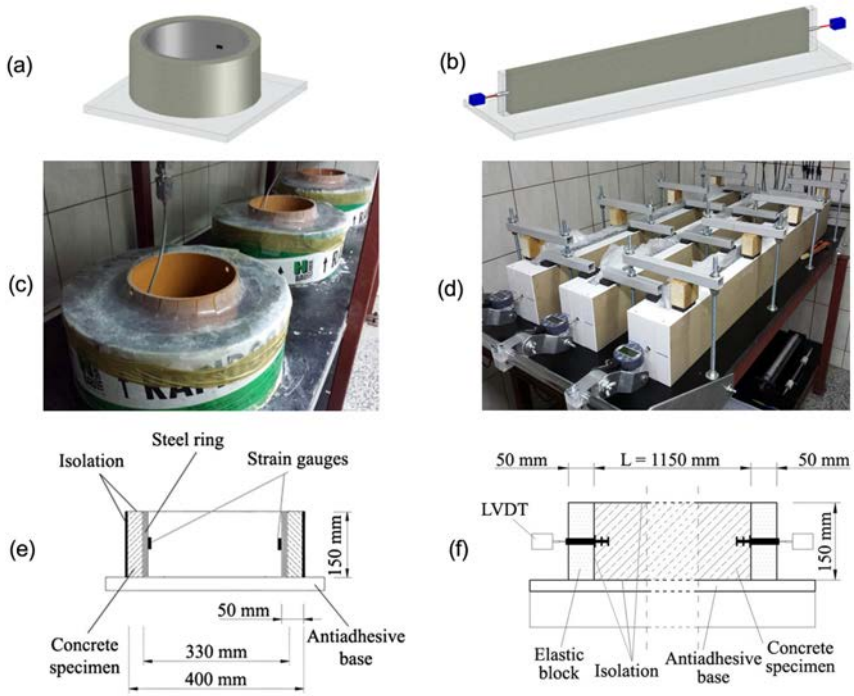

Fig. 2. Laboratory tests: (a) schematic restrained ring specimen; (b) schematic linear specimen with matching geometry; (c) view of the restrained ring test during research; (d) view of the free autogenous shrinkage during research; (e) cross-section and description of the specimen of the method ASTM C1581M-16; (f) cross-section and description of the specimen using linear specimens

circumferential strain of the ring specimens, which allows one to correlate this strain to the maximum circumferential stresses determined according to the Equation (2.1) [18].

$$\sigma_{t,c}(t) = -\varepsilon_{\text{steel}}(t) \cdot E_s \cdot \frac{R_{\text{OS}}^2 - R_{\text{IS}}^2}{2R_{\text{OS}}^2} \cdot \frac{R_{\text{OC}}^2 + R_{\text{OS}}^2}{R_{\text{OC}}^2 - R_{\text{OS}}^2} \quad \text{(MPa)} \tag{2.1}$$

where: $\sigma_{t,c}$ – actual circumferential maximum tensile stress over time t, $\varepsilon_{\text{steel}}$ – circumferential strain of the steel ring at any time, t; E_s– modulus of elasticity of the steel ring; R_{OS} – outer radius of the steel ring; R_{IS} – inner radius of the steel ring; R_{OC} – outer radius of the concrete ring specimen.

The elimination of the effect of drying from the vertical surface in acc. with C1581 changed the distribution of tensile stresses in the cross section of the concrete ring specimen. The maximum stresses were generated on the inner surface of the concrete ring specimen in contact with the steel ring and they determined the development of microcracks and, as a result, the cracking of the specimen. The deformation of linear specimens was measured at two free ends with the use of digital gauge e.g. linear variable differential transformer (LVDT). The actual shrinkage strains of the linear specimens were calculated acc. to

Equation (2.2).

$$\varepsilon_{au}(t) = \frac{\Delta l_{1,t} + \Delta l_{2,t}}{L} \cdot 10^6 \ (\mu m/m) \tag{2.2}$$

where: ε_{au} – value of the linear autogenous shrinkage of the linear specimen over time t, $\Delta l_{1,t}$, $\Delta l_{2,t}$ – measured displacement of the specimen at the 1st and 2nd free ends, after time t with regard to the first measurement; L – length of the prismatic specimen.

Measurement of steel ring strains and free, linear autogenous shrinkage started from molding the specimens until either cracking of the ring specimen or until a concrete age of 28 days. For each cement composite, these two tests were performed simultaneously on material sampled from the same batch. A view of the steel ring test setup is shown in Fig. 2c and Fig. 2d. The setup to measure the free autogenous shrinkage using linear specimens is shown in Fig. 2e and Fig. 2f.

In both tests, the specimens were sealed from any moisture loss throughout the entire testing period. The test stands containing all specimens were stored in a climatic room that maintained a constant temperature of $20 \pm 2^{\circ}C$. All measurements were electronically recorded at a constant interval of 5 minutes. All specimens had the same small cross-section (35×150 mm); therefore, the temperature development was limited and had similar effects on both tests. All restrained ring test stands were fabricated and before testing began, each ring test stand was calibrated to ensure that accurate measurements are obtained. The calibration of the steel rings, with strain gauges glued on the inner ring face, included pneumatic method as detailed in [25]. To ensure repeatability of results of the three linear test stands, their form tightness was verified and a series of tests to determine how to minimize the effects of friction were performed to verify that accurate strain measurements are obtained in initial calibration specimens.

3. Results and discussion

3.1. Physical properties

All the high-performance composites considered were designed with self-compacting properties. Measured parameters for the self-consolidating mortars that include flowability (Slump flow), viscosity (V-funnel), visual stability index (VSI) [2]. Tests for volumetric density according to EN 12390-7, compressive strength (f_c) performed on $100 \times 100 \times 100$ mm specimens according to EN 12390-3, and splitting tensile strength (f_{ct}) performed on $150 \times 50 \times 100$ mm specimens according to EN 12390-6 were performed. Note that the geometry of the splitting tensile strength specimens was different from what is usually used, because this size was selected to match the cross-section size of the ring test specimens to allow the comparison of splitting tensile strength results with the development of tensile stresses at cracking of the ring specimens according to ASTM C1581M-16. In order to allow for the direct comparison of the results from both tests, the width of the specimens should be the same and their height similar [18]. Strength tests were performed on three specimens at concrete ages of 2, 7 and 28 days. Table 5 shows the strength and volume

Table 5. Physical parameters of the tested cement composites

Parameter	Age (days)	M-0.34-NWA	M-0.225-NWA	M-0.225-LWA	C-0.225-NWA	C-0.28-NWA	C-0.28-LWA
Density; σ (kg/m^3)	28	2220; 12	2260; 15	1870; 8,5	2340; 15	2320; 10	1780; 5,0
$f_{c,100\times100}$; σ (MPa)	1	45.7; 1.21	71.3; 2.47	44.6; 2.64	67.2; 2.19	60.1; 1.32	24.0; 1.34
	3	57.1; 2.14	84.7; 2.85	59.1; 2.12	83.0; 1,32	75.1; 1.88	44.0; 1.79
	7	60.9; 2.41	98.0; 3.21	65.9; 1.44	96.3; 1.67	87.2; 2.10	48.6; 2.21
	28	76.7; 3.15	110.1; 2.71	71.9; 2.17	107.5; 2.35	105.6; 2.12	55.0; 2.55
$f_{ct,sp50\times150}$; σ (MPa)	1	3.74; 0.14	5.97; 0.59	3.80; 0.40	5.42; 0.58	5.21; 0.78	2.82; 0.53
	3	4.41; 0.75	6.76; 0.35	4.02; 0.84	6.58; 0.52	6.21; 0.18	3.12; 0.29
	7	5.15; 0.23	7.43; 0.19	4.38; 0.21	7.34; 0.49	6.50; 0.24	3.47; 0.79
	28	7.04; 0.67	8.85; 0.24	4.95; 0.31	8.71; 0.94	7.68; 0.43	4.39; 0.40

density results together with the standard deviation (σ) of the tests conducted at each age. At a concrete age of 28 days, HVSI classification in accordance with AASHTO PP-58 was performed on both linear and ring specimens. All sections of each composite were characterized as HVSI1.

3.2. Autogenous shrinkage

The analysis of free and restrained deformations was performed for the period that started at final setting until a specimen age of either 28 days or until cracking occurred. The strain recorded in the period from specimen casting to the time of final setting was reset to zero because autogenous shrinkage starts at final setting [18]. The final setting time of each test was estimated according to the inflection point of the development of autogenous strain for each composites in the first 24 hours of maturation [26]. For a more precise analysis, the correlation between autogenous shrinkage and tensile stress was individually compiled for mortars as shown in Fig. 3 and for concretes in Fig. 4. The development of strains and stresses is presented as the average measured from the three specimens for each cementitious material. As an example, the development of autogenous shrinkage and tensile stress results for M-0.34-NWA and C-0.225-NWA are presented in Fig. 3 and Fig. 4, respectively, for two time periods that first cover the first 24 h and 28 days. The measured of strains and stresses of the remaining cement composites is presented for the full 28-day measurement period.

The mortar with the lowest w/b ratio of 0.225 (M-0.225-NWA) and did not include any internal curing had the highest autogenous shrinkage after 24 h and after 28 days, which is as expected. The rapid rate of early-age development and high autogenous shrinkage value is a result of the low water content resulting in self-desiccation with the progress of hydration and the highest capillary pressure in the pores. Therefore, it resulted in exceeding the strength of the material and cracking after just 4.2 days in the restrained ring test, which is the earliest that cracking occurred in any of the ring test specimens. When analyzing

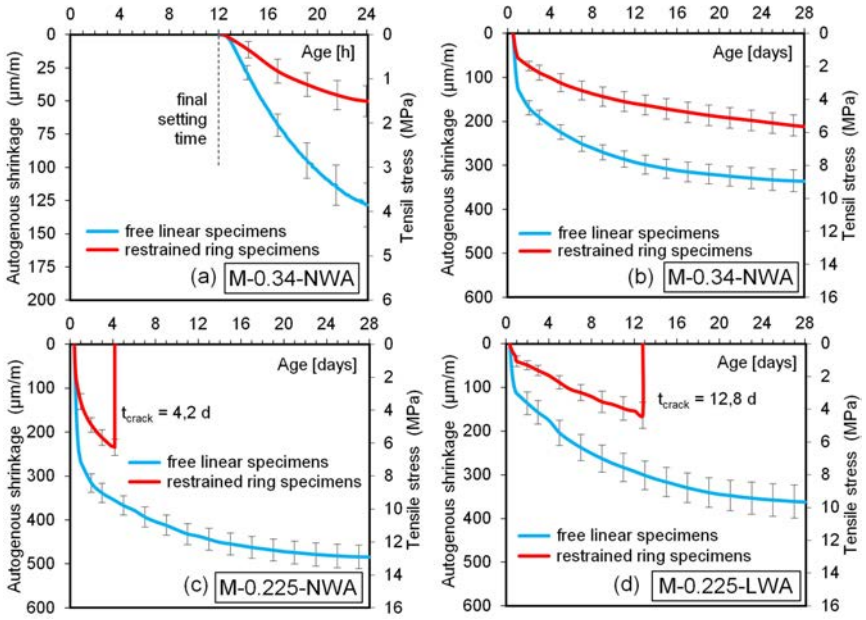

Fig. 3. Development of strain and stress measured in all mortars: a) M-0.34-NWA – 24h; b) M-0.34-LWA – 28 d; c) M-0.225-NWA – 28 d; d) M-0.225-LWA – 28 d

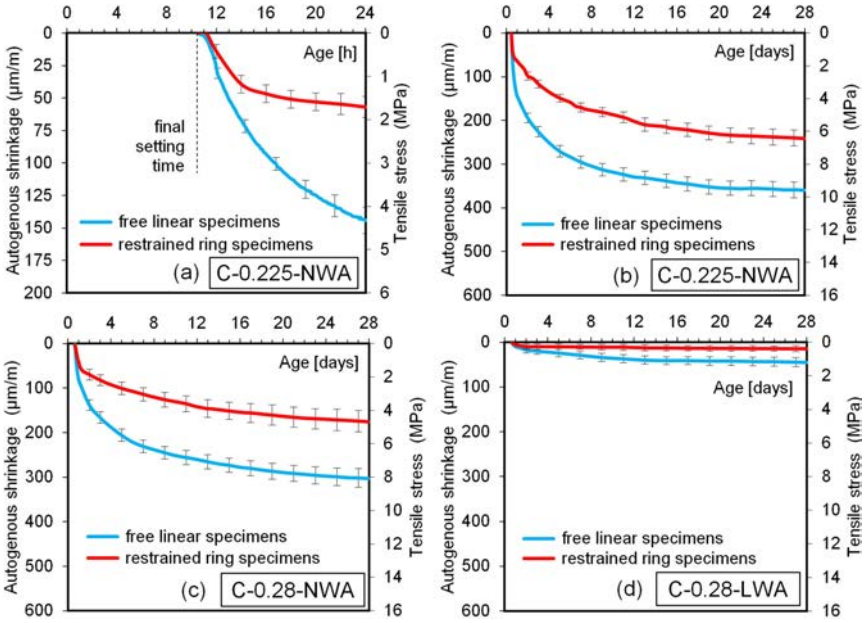

Fig. 4. Development of strain and stress measured in all concretes: a) C-0.225-NWA – 24h; b) C-0.225-NWA – 28 d; c) C-0.28-NWA – 28 d; d) C-0.28-LWA – 28 d

M-0.225-NWA and M-0.225-LWA, it can be seen that the method of using fine lightweight aggregate soaked with an additional internal curing water in 25% of the mass of the mixing water, was effective in delaying cracking in the ring test. The use of internal curing reduces the 28-day autogenous shrinkage by 25% and increases the mortar cracking resistance by 8.6 days. The fine lightweight aggregate was not able to store enough internal curing water to prevent cracking of the mortar over the 28-day testing period. When comparing M-0.34-NWA and M-0.225-NWA, it can be seen that increasing the w/b ratio from 0.225 to 0.34 reduces the 28-day autogenous shrinkage by over 30% and the mortar with a w/c of 0.34 did not crack over the 28 days testing period. Mortar M-0.34-NWA did not crack, but had a 20% lower splitting tensile strength after 28 days when compared to M-0.225-NWA. The use of fine lightweight aggregate in M-0.225-LWA lowered the value of splitting tensile strength by nearly 45% when compared to M-0.225-NWA as shown in Table 5. The use of fine lightweight granulated fly ash aggregate decreased the splitting strength and resulted in earlier cracking.

The concrete with the lowest w/b ratio of 0.225 (C-0.225-NWA) had the highest autogenous shrinkage after 24 hours and after 28 days, which is as expected. When analyzing C-0.28-NWA and C-0.225-NWA, increasing the w/b ratio from 0.225 to 0.28 reduces the 28-day autogenous shrinkage by over 15%. When comparing concrete with a w/b ratio of 0.28 (C-0.28-NWA) versus one with the same w/b ratio of 0.28 but containing internal curing water (C-0.28-LWA) in Fig. 4, is can be seen that the mixture with internal curing had much less autogenous shrinkage and restrained concrete stress as measured in the steel ring test. Additional replacement of coarse granite aggregate with soaked coarse lightweight aggregate (C-0.28-LWA) with an additional internal curing water in 70% of the mass of the mixing water, was very effective to mitigate autogenous shrinkage. The availability of loosely bound internal water in the pores of granulated fly ash was desorbed to the hydrating paste upon self-desiccation, which reduced the autogenous shrinkage of C-0.28-LWA by six times when compared to that of C-0.28-NWA that did not contain internal curing water. The graphs shown in Fig. 5 summarizes the material effect on reducing autogenous shrinkage and minimizing susceptibility to cracking of the tested cementitious composites.

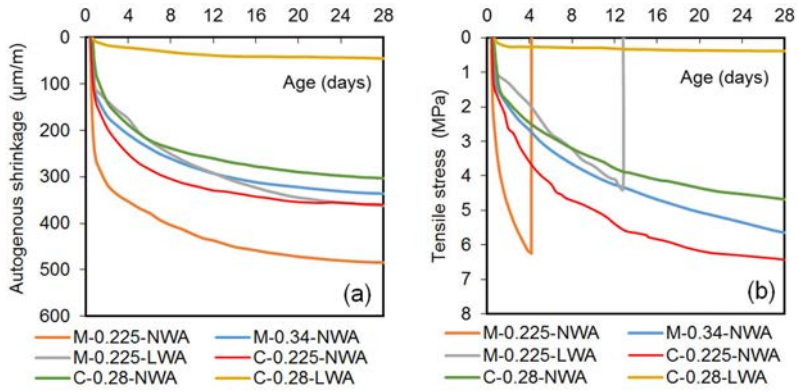

Fig. 5. Development of parameters of tested cement composites: a) autogenous shrinkage – free linear specimens; b) tensile stress – restrained ring test

3.3. Cracking risk

Comparison of measured concrete tensile stress ($\sigma_{t,c}$) determined with Eq. (2.1) divided by the splitting tensile strength (f_{sp}) of the concretes over time allows one to assess the cracking risk (θ_{CR}) in accordance with Equation (3.1) [18, 27].

$$\theta_{CR}(t) = \frac{\sigma_{t,c}(t)}{f_{sp}(t)} \quad (\%) \tag{3.1}$$

The value of $f_{sp}(t)$ over time was determined from the regression analysis of the splitting tensile test results and are presented in Fig. 6. It can be seen from the high coefficients of determination (R^2) that the best-fit curves obtained from the regression analysis are a good fit for the measured results. In the cracking ring test, comparing the cracking risk (θ_{CR}) is particularly meaningful when a crack is not registered in a test of a cement composite. To assess the cracking risk the following four relationships were analyzed: 1) tensile stress versus splitting tensile strength development; 2) tensile stress versus autogenous shrinkage development; 3) cracking risk versus autogenous shrinkage development; and 4) cracking risk development versus specimen age. The results of these comparisons are presented individually for mortars in Fig. 7 and for concretes in Fig. 8. This comparison allows one to evaluate the impact of internal curing to mitigate the cracking risk.

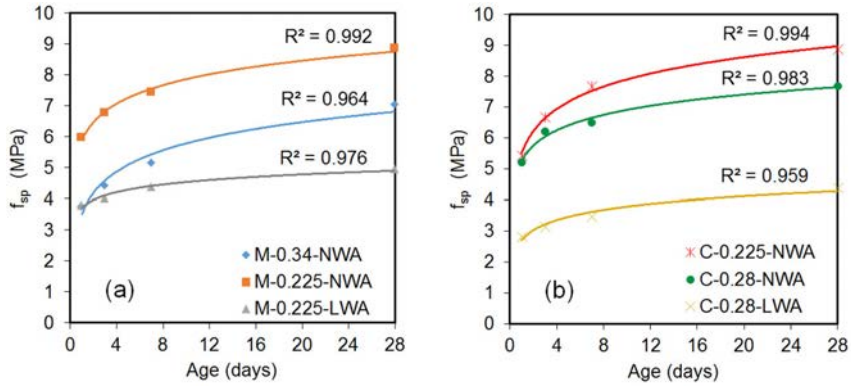

Fig. 6. Regression fits for age-dependent splitting tensile strength: a) mortars; b) concretes

High-performance mortar M-0.225.NWA cracked after just 4.2 days which is the earliest of all the mixtures tested in this study. Mortar M-0.34-NWA with a higher w/b ratio did not crack in the 28-day evaluation period, which reveals that an increase in the w/b ratio is an effective way to reduce influence of autogenous shrinkage in mortars. M-0.225-LWA that contained soaked fine lightweight aggregate that provided internal curing water delayed cracking by more than 8 days when compared to M-0.225.NWA. The cracking risk of M-0.34-NWA and M-0.225-LWA in Fig. 7d are very similar during the first 7 days; however, thereafter the cracking risk of M-0.34-NWA becomes less and remains low through the 28-day test period. On the other hand, for this specific granulated fly ash, the internal curing water provided did not mitigate the autogenous shrinkage (as shown in Fig. 7c) and also

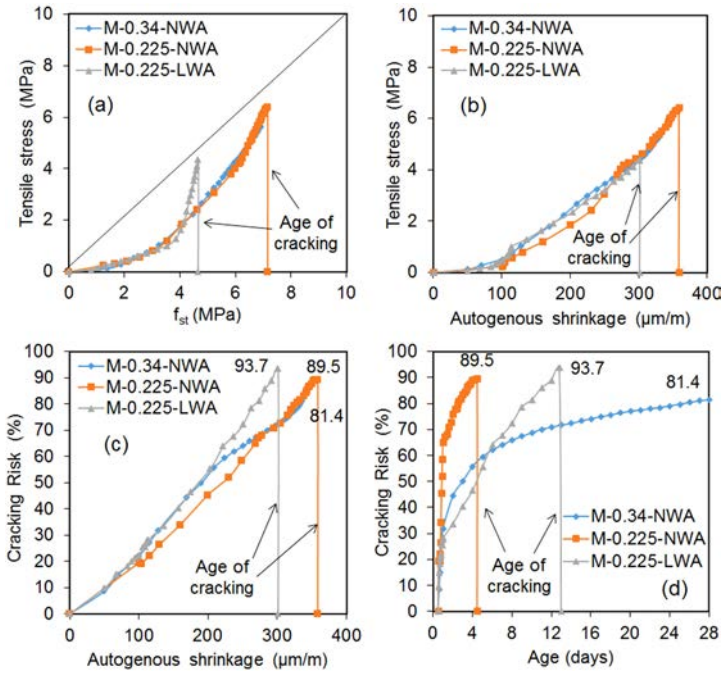

Fig. 7. Evaluation of cracking risk for cement mortars: a) $\sigma_{t,c}/f_{st}$; b) $\sigma_{t,c}/\varepsilon_{au}$; c) CR/$\varepsilon_{au}$; d) CR/age

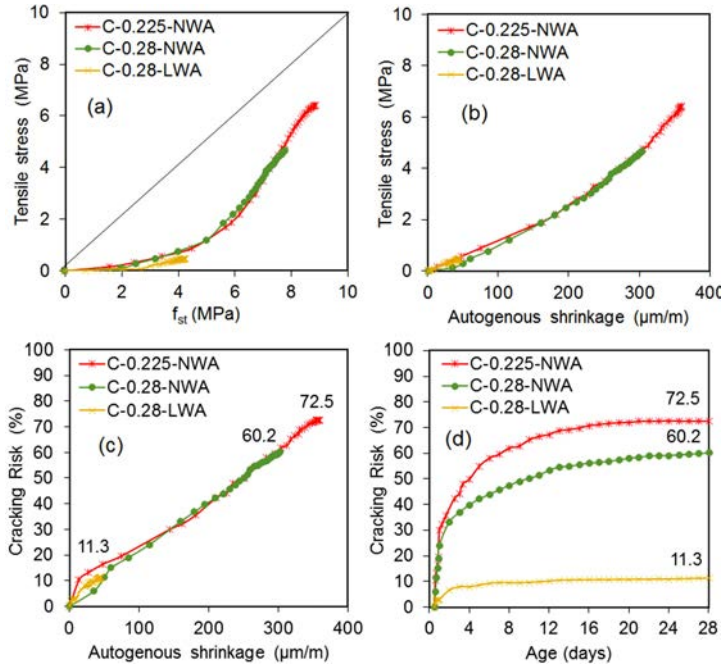

Fig. 8. Evaluation of cracking risk of concretes: a) $\sigma_{t,c}/f_{st}$; b) $\sigma_{t,c}/\varepsilon_{au}$; c) CR/$\varepsilon_{au}$; d) CR/age

caused a reduction in the mortar tensile strength which resulted in cracking after 12.8 days. Cracking in two of three analyzed mortars occurs before reaching CR = 100%, which is similar as found by other research studies [18, 28].

None of the concretes cracked within a concrete age of 28 days. As shown in Fig. 8d, an increase in w/b ratio from 0.225 to 0.28 for the normalweight aggregate concretes reduced cracking risk by approximately 12% at 28 days. As shown in Fig. 8c the use of coarse lightweight aggregate soaked with water resulted in a significant reduction in autogenous shrinkage which indicates that effective internal curing was provided. When comparing concrete C-0.28-LWA to C-0.28-NWA it can be seen in Fig. 8d that the use of internal curing leads to a significant reduction (more than 5 times less) in cracking risk. The use of coarse granulated fly ash aggregate soaked with water significantly lowers the cracking risk due to restrained autogenous shrinkage stresses.

4. Conclusions

Analyses described in this paper proved that lowering w/b ratio increases the cracking risk of cement composites due to autogenous shrinkage. Reducing the b/a ratio, which is characteristic of concrete, reduces the value of autogenous shrinkage and reduces the risk of cracking. Due to limited reservoir of stored water in the pores of granulated fly ash used as fine lightweight aggregate in this study, this specific aggregate minimally extended the time to cracking and significantly reduced the concrete strength. Use of soaked granulated coarse lightweight aggregate in cementitious composites provided minimizes both, autogenous shrinkage and cracking risk but also reduces strength parameters.

Authorship contribution statement

Adam Zieliński: Data curation, Conceptualization, Methodology, Validation, Formal analysis, Writing – original draft. Anton Schindler: Data curation, Validation, Writing – review and editing. Maria Kaszyńska: Data curation, Writing – review and editing.

References

[1] A.K. Schindler, D. Trejo, and R.W. Barnes, *Self-consolidating concrete for prestress precast applications*. Special Publication 247, American Concrete Institute, 2007.

[2] G. de Schutter, *Self-compacting concrete*. Caithness u.a: Whittles, 2008.

[3] R. Siddique, *Self-compacting concrete: materials, properties and applications*. Woodhead Publishing, 2019.

[4] H. Okamura and M. Ouchi, "Self-compacting high performance concrete", *Progress in Structural Engineering and Materials*, vol. 1, no, 4, pp. 378–383, 1998, doi: 10.1002/pse.2260010406.

[5] L. Barcelo, M. Moranville, and B. Clavaud, "Autogenous shrinkage of concrete: A balance between autogenous swelling and self-desiccation", *Cement and Concrete Research*, vol. 35, no. 1, pp. 177–183, 2005, doi: 10.1016/j.cemconres.2004.05.050.

[6] P. Lura, O.M. Jensen, and J. Weiss, "Cracking in cement paste induced by autogenous shrinkage", *Materials and Structures*, vol. 42, no. 8, pp. 1089–1099, 2009, doi: 10.1617/s11527-008-9445-z.

[7] E-i. Tazawa, *Autogenous shrinkage of concrete proceedings of the workshop by JCI*. London: E & FN Spon, 1999.

[8] P. Gao, T. Zhang, R. Luo, J. Wei, and Q. Yu, "Improvement of autogenous shrinkage measurement for cement paste at very early age: Corrugated tube method using non-contact sensors", *Construction and Building Materials*, vol. 55, no. 6, pp. 57–62, 2014, doi: 10.1016/j.conbuildmat.2013.12.086.

[9] E-i. Tazawa and S. Miyazawa, "Estimation of autogenous shrinkage of concrete", *Doboku Gakkai Ronbun-shu*, vol. 571, pp. 211–219, 1997, doi: 10.2208/jscej.1997.571_211.

[10] E-i. Tazawa and S. Miyazawa, "Influence of cement and admixture on autogenous shrinkage of cement paste", *Cement and Concrete Research,* vol. 25, no. 2, pp. 281–287, 1995, doi: 10.1016/0008-8846(95)00010-0.

[11] P. Nath and P. Sarker, "Effect of fly ash on the durability properties of high strength concrete", *Procedia Engineering*, vol. 14, no. 2, pp. 1149–1156, 2011, doi: 10.1016/j.proeng.2011.07.144.

[12] D. Ballekere Kumarappa, S. Peethamparan, and M. Ngami, "Autogenous shrinkage of alkali activated slag mortars: Basic mechanisms and mitigation methods", *Cement and Concrete Research*, vol. 109, pp. 1–9, 2018, doi: 10.1016/j.cemconres.2018.04.004.

[13] E. Holt, *Early age autogenous shrinkage of concrete*. Technical Research Centre of Finland, 2001.

[14] J. Liu, Z. Ou, J. Mo, Y. Wang, and H. Wu, "The effect of SCMs and SAP on the autogenous shrinkage and hydration process of RPC", *Construction and Building Materials*, vol. 155, no. 7, pp. 239–249, 2017, doi: 10.1016/j.conbuildmat.2017.08.061.

[15] J. Saliba, E. Rozière, F. Grondin, and A. Loukili, "Influence of shrinkage-reducing admixtures on plastic and long-term shrinkage", *Cement and Concrete Composites*, vol. 33, no. 2, pp. 209–217, 2011, doi: 10.1016/j.cemconcomp.2010.10.006.

[16] H. Liu, G. Duan, and J. Zhang, "Drying shrinkage and creep properties of self-compacting concrete with expansive agent and viscosity modified admixture", *Archives of Civil Engineering*, vol. 68, no. 3, pp. 539-551, 2022, doi: 10.24425/ace.2022.141901.

[17] M. Kaszyńska and A. Zielinski, "Effect of lightweight aggregate on minimizing autogenous shrinkage in self-consolidating concrete", *Procedia Engineering*, vol. 108, no. 3, pp. 608–615, 2015, doi: 10.1016/j.proeng.2015.06.186.

[18] A.B. Hossain and J. Weiss, "Assessing residual stress development and stress relaxation in restrained concrete ring specimens", *Cement and Concrete Composites*, vol. 26, no. 5, pp. 531–540, 2004, doi: 10.1016/S0958-9465(03)00069-6.

[19] J. Weiss, W. Yang, and S.P. Shah, "Influence of specimen size/geometry on shrinkage cracking of rings", *Journal of Engineering Mechanics,* vol. 126, no. 1, 2000, doi: 10.1061/(ASCE)0733-9399(2000)126:1(93).

[20] B.E. Byard, A.K. Schindler, and R.W. Barnes, "Early-age cracking tendency and ultimate degree of hydration of internally cured concrete", *ASCE Journal of Materials in Civil Engineering*, vol. 24, no. 8, pp. 1025–1033, 2012, doi: 10.1061/(ASCE)MT.1943-5533.0000469.

[21] Z. He, X. Zhou, and Z. Li, "New experimental method for studying early-age cracking of cement-based materials", *ACI Materials Journal,* vol. 101, no. 1, pp. 50–56, 2004.

[22] Y. Liu, A.K. Schindler, and J.S. Davidson, "Finite-element modeling and analysis of early-age cracking risk of cast-in-place concrete culverts", *Journal of the Transportation Research Board*, vol. 2672, no. 27, pp. 24–36, 2018, doi: 10.1177/0361198118774157.

[23] A. Radlińska, M. Kaszyńska, A. Zieliński, and H. Ye, "Early-age cracking of self-consolidating concrete with lightweight and normal aggregates", *ASCE Journal of Materials in Civil Engineering*, vol. 30, no. 10, 2018, doi: 10.1061/(ASCE)MT.1943-5533.0002407.

[24] *Test method No.: NY 703-19 E Moisture content of lightweight fine aggregate*. New York State Department of Transportation, Materials Bureau, 2008.

[25] A. Zieliński and M. Kaszyńska, "Calibration of steel rings for the measurement of strain and shrinkage stress for cement-based composites", *Materials*, vol. 13, no. 13, 2020, doi: 10.3390/ma13132963.

[26] J.R. Tenório Filho, M.A. Pereira Gomes de Araújo, D. Snoeck, and N. de Belie, "Discussing different approaches for the time-zero as start for autogenous shrinkage in cement pastes containing superabsorbent polymers", *Materials*, vol. 12, no. 18, art. no. 2962, 2019, doi: 10.3390/ma12182962.

[27] K.A. Riding, J.L. Poole, A.K. Schindler, M.C. Juenger, and K.J. Folliard, "Statistical determination of cracking probability for mass concrete", *Journal of Materials in Civil Engineering*, vol. 26, no. 9, 2014, doi: 10.1061/ (ASCE)MT.1943-5533.0000947.

[28] K. van Breugel, S.J. Lokhorst, "Stress-based crack criterion as a basis for prevention of through-cracks in concrete structures at early ages", in *International RILEM Conference on Early Age Cracking in Cementitious Systems*. RILEM, 2003, pp. 229-236.

Ryzyko pękania wysokowartościowych kompozytów cementowych z i bez nasączonego kruszywa lekkiego z powodu ograniczenia skurczu autogenicznego

Słowa kluczowe: skurcz autogeniczny betonu, ryzyko pękania betonu, ograniczony skurcz autogeniczny, pękanie betonu w młodym wieku, pielęgnacja wewnętrzna

Streszczenie:

Z powodu dużej ilości spoiwa i niskiego wskaźnika woda-cement, wysokowartościowe kompozyty cementowe mają wysoką wytrzymałość na ściskanie i szczelną mikrostrukturę. Zewnętrzna pielęgnacja jest niewystarczająca, ponieważ nie może dotrzeć do wewnętrznej struktury materiału, co pozwala na wystąpienie skurczu autogenicznego. Brak zabezpieczenia materiału przed skurczem autogenicznym i wysoki poziom ograniczenia odkształceń powodują mikropęknięcia wokół sztywnych ośrodków materiałowych (kruszywo, pręty zbrojeniowe). W konsekwencji zjawisko prowadzi do propagacji mikropęknięć wewnętrznych do strefy powierzchniowej i utraty trwałości betonu. Jednym ze sposobów minimalizacji skurczu autogenicznego jest pielęgnacja wewnętrzna. Zastosowanie namoczonego kruszywa lekkiego w celu zminimalizowania ryzyka pękania jest nie zawsze wystarczające. Zbadano i oceniono kinetykę sorpcji i desorpcji drobnego i grubego kruszywa lekkiego z granulowanego popiołu lotnego. W artykule przedstawiono korelację między rozwojem liniowego skurczu autogenicznego a naprężeniami rozciągającymi w teście pierścienia ograniczającego wg ASTM C1581. Zbadano i przeanalizowano serię próbek liniowych o przekroju poprzecznym i długości dostosowanych do geometrii próbek pierścieniowych. Określenie maksymalnych naprężeń rozciągających wywołanych przez ograniczony skurcz autogeniczny w teście pierścieniowym wraz z przybliżonym rozwojem wytrzymałości na rozciąganie kompozytów cementowych użyto do oceny rozwoju ryzyka pękania w czasie. Badania objęły wysokowartościowe betony i zaprawy z kruszywem naturalnym i kruszywem lekkim nasączonym wodą. Zastosowanie w kompozytach cementowych grubego kruszywa lekkiego zminimalizowało zarówno rozwój skurczu autogenicznego i ryzyko pękania.

Received: 2023-06-07, Revised: 2023-08-22